Positron Emission Tomography of Fluorine-18-Deoxyglucose and Image-Guided Phosphorus-31 Magnetic Resonance Spectroscopy in Brain Tumors

W.-D. Heiss, W. Heindel, K. Herholz, J. Rudolf, J. Bunke, J. Jeske, and G. Friedmann

Max-Planck-Institut für Neurologische Forschung, Klinik für Neurologie und Psychiatrie—Neurologie—and Radiologisches Institut der Universität zu Köln, Köln Lindenthal, Federal Republic of Germany

Positron emission tomography (PET) of 2(^{18}F)-fluoro-2-deoxy-D-glucose (FDG) and volume-selective phosphorus-31 magnetic resonance spectroscopy (^{31}P-MRS) are methods used to assess the energy metabolism of the brain. Both methods were studied with respect to their contribution to differential diagnosis in 23 patients with various brain tumors. The various neuroectodermal tumors differed with respect to their metabolic rate for glucose (MRGL). Benign and malignant tumors could be better differentiated by using tumor metabolism relative to contralateral brain and by evaluating heterogeneities in tumors. Low-grade gliomas usually showed normal ^{31}P-MR spectra; high-grade gliomas were characterized by reduced and often split phosphodiester peaks and alkaline pH. Meningiomas, which had variable MRGL, typically showed extremely low phosphocreatine levels, reduced phosphodiesters, and alkaline pH. We concluded that FDG-PET and ^{31}P-MRS examine different aspects of tumor metabolism. Therefore, both can contribute independently and complementarily to the differential diagnosis of brain tumors.

J Nucl Med 1990; 31:302-310

Several studies of metabolic rate for glucose (MRGL) with positron emission tomography (PET) of flourine-18-2-fluoro-2-deoxy-D-glucose (FDG) have shown a positive correlation between glioma grade and glycolytic activity (*1*). These data supported Warburg's suggestion (*2*) that the rate of glycolysis in tumors increases with higher degree of malignancy. Despite a large variability of MRGL in various tumors of one type and a considerable overlap of the glucose uptake values of tumors belonging to different biologic groups (*1*, *3*, *4*), FDG-PET is considered by some authors (*1*, *5*) a remarkably effective, noninvasive method of differentiating primary brain tumors, and was found in some instances to predict survival better than histologic classification (*3*). However, other authors (*6*, *7*) could not confirm a close association between tumor grade and MRGL.

With the advent of magnetic resonance (MR) imaging and the development of wide bore magnets it has become possible to observe MR spectra in intact animals and recently in man (*8*, *9*). Phosphorus-31 MRS can provide additional metabolic information on the cellular phosphate compounds and pH of tumors in situ. It has demonstrated differences in the level of phosphate metabolites between intracranial tumors and healthy brain tissue and among different tumors (*10*, *11*). Thus, FDG-PET and ^{31}P-MRS apparently examine different aspects of tumor energy metabolism. This pilot study was designed to examine whether combination of the two methods may actually yield complementary information on tumor metabolism and whether that may contribute to differential diagnosis and tumor grading. Preliminary results of this study have been reported at the SNM Meeting 1988 (*12*).

MATERIALS AND METHODS

Patients

Twenty-four subjects, 15 males and 9 nonpregnant females, age 23–71 yr (mean 46 yr) were entered into the protocol. All were referred to our institution for evaluation of an intracranial space-occupying lesion suspected of being a brain tumor. All patients were able to give informed consent to the proposed procedures. Besides the routine clinical examinations and tests all patients had x-ray CT scans before and after i.v. application of contrast material. In most patients, MRI and spectroscopy (MRS) and PET were performed before any specific tumor therapy other than corticosteroids was initiated. PET and MRS followed each other usually within five days. With the exceptions of four inoperable brain tumors presenting with the clinical and radiologic characteristics of glioblastomas, all diagnoses were histologically verified. Histological classification according to current WHO criteria was based on speci-

Received July 20, 1989; revision accepted Oct. 31, 1989.

For reprints contact: W.D. Heiss, MD, Max-Planck-Institut für neurologische Forschung, Klinik für Neurologie und Psychiatrie, Neurologie, Joseph-Stelzmann-Str. 9, 5000 Köln 41, FRG.

mens obtained during open-tumor resection, by open biopsy or by stereotaxic biopsy. The groups according to tumor type are summarized in Table 1.

PET Measurement

Approximately 185 MBq (5 mCi) FDG, synthesized according to Ido et al. (*13*) and Ehrenkaufer et al. (*14*) were injected with an i.v. bolus. Blood sampling and scanning procedures in the Scanditronix PC 384 (Uppsala, Sweden) tomograph with seven slices and standard image reconstruction software are described in a previous paper (*15*). Metabolic images were computed using a K_1–k_3 optimization procedure (*16*) and a lumped constant of 0.42. Circular or rim-shaped regions including the main bulk of solid tumor ("tumor core") as judged on the basis of corresponding x-ray CT scans and a large region comprising the whole area of possible tumor infiltration (gross tumor) were superimposed on the metabolic images and mean values were calculated within each region. If the tumor extended across several slices, averages weighted by region size were calculated. In addition, metabolic rates were determined separately in cystic or necrotic tumor parts in those cases where a clear delineation was possible. Furthermore, regions of interest of various geometric shapes adapted to brain anatomy were placed over all normal brain areas using a computer-assisted mapping procedure (*17*). Displacement of normal brain structures by tumor mass effects was accounted for by interactive correction of region placement. Metabolic rates in patients were related to normative values obtained in a sample of 26 age-matched healthy persons (mean age 47, range 21–72 yr). Normal white matter in the semioval center served as a reference for tumor MRGL.

Magnetic Resonance Studies

Combined MRI and MRS were performed on a 1.5-T whole-body MR system (Gyroscan S15, Philips, Eindhoven, Netherlands) operating at 64 MHz for ^1H and 25.9 MHz for ^{31}P. Phosphorus-31 spectra were obtained with a small phosphorus-tuned head coil, which was placed with orthogonal orientation inside the usual proton imaging head coil. The latter was used for obtaining routine proton images to locate the tumor and for shimming. Spatially resolved phosphorus spectra were then acquired from block-shaped volumes (>3×3×3 cm) centered on the tumors using a modified version of the Isis technique (*18*) as described by den Hollander and Luyten (*19*). The size of this volume corresponded roughly to the "gross tumor" regions in PET. In several cases, a double-volume technique permitted simultaneous acquisition of ^{31}P spectra from control tissue. Normative data had been obtained in 30 young healthy volunteers in a previous study (*11*) using the same technique.

RESULTS

Normal values

The marked volume necessary to obtain a reliable ^{31}P spectrum is rather large containing various morphologic tissue compartments with widely differing MRGL (between 15 μmol/100 g/min for white matter/centrum semiovale and ~ 40 μmol/100 g/min for grey matter in basal ganglia/thalamus and cortex (*15*)). Mean cerebral hemispheric metabolism in the present reference sample of 26 age-matched healthy persons was 34.2 ± 4.0 (s.d.) μmol/100 g/min with MRGL in the centrum semiovale—also used as a reference for gliomas with respect to their histologic origin—of 17.9 ± 2.6 μmol/100 g/min. From the volumes placed in the center of forebrain hemispheres, normal ^{31}P spectra were obtained with the typical seven peaks for beta, alpha, and gamma adenosine triphosphate (ATP), phosphocreatine (PCr), phosphodiesters (PDE), inorganic phosphate (Pi), and phosphomonoesters (PME). In studies of the healthy volunteers, the peak of β -ATP was especially constant with small variations of the other peaks, mainly marked in the PME. However, the variation of relative height of the peaks in relation to the β-ATP usually did not exceed ±10% (*20*), and repeat studies in individual volunteers usually yielded highly comparable spectra (*11*). Brain pH, determined from the position of the inorganic phosphate peak relative to the phosphocreatine peak (*21*) using the titration curve of Petroff et al. (*22*), averaged 7.01 ± 0.06 in these volunteers (*11*).

MRGL in Tumors

A large variability of MRGL was found among the tumors of each histologic group (Table 2), but also the metabolic rates within individual tumors of most patients showed considerable local differences. Grade II astrocytomas (Fig. 1) had metabolic rates between 16.7 and 25.9 μmol/100 g/min, with a mean of 19.3. These values were close to the MRGL in contralateral white matter (oval center) of patients (17.7, s.d. 3.1) and normal controls (17.9, s.d. 2.6). There was a broad overlap with tumor core MRGL in grade III gliomas (range 16.8 to 30.0, mean 25.2 μmol/100 g/min) (Fig. 2) and glioblastomas (range 14.2 to 26.3, mean 19.3 μmol/100 g/min). Metabolism was very inhomogene-

TABLE 1
Patients with Various Brain Tumors Included in the FDG-PET and ^{31}P-MRS Study

Tumor Group	N	Age (range in years)	Diagnosis by Histology	Diagnosis by Radiology	Clinical course: Stable n (since mo)	Clinical course: Recurrency n (after mo)	Clinical course: Death n (after mo)
Astrocytoma II	6	24.9–40.5	6	—	4 (9–26)	2 (12)	—
Glioma III	4	24.6–48.8	4	—	1 (9)	—	3 (4–19)
Glioblastoma	10	46–65	6	4	4 (6–14)	1 (12)	5 (2–9)
Meningioma	3	23, 70, 72	3	—	3 (8–10)	—	—

TABLE 2
Average Quantitative PET and MRS Results in Tumor Groups (mean values s.d.)

Histologic diagnosis	n	MRGL (μmol/100 g/min) gross tumor	MRGL (μmol/100 g/min) tumor core	Rel. MRGL contralateral hemisphere	Rel. MRGL tumor core	Tissue pH tumor	Tissue pH contralateral hemisphere*
Astrocytoma Grade II	6	23.1/3.9	19.3/3.4	36.1/5.7	0.54/0.06	7.01/0.09	7.05/0.05
Glioma Grade III	4	23.2/4.1	25.2/6.2	31.3/4.2	0.80/0.13	7.15/0.08	7.01/0.03
Glioblastoma Grade IV	10	18.6/3.1	19.3/3.7	28.3/5.3	0.69/0.16	7.18/0.09	7.11/0.09
Meningioma	3	30.7/8.5	31.8/9.3	37.3/5.9	0.86/0.25	7.16/0.12	7.10

* pH values in contralateral hemisphere were available in 17 cases only.

ous in most glioblastomas (Fig. 3) with peak values within the tumor core as high as 55 μmol/100 g/min. Areas with very low MRGL, on average 3.9 μmol/100 g/min (s.d. 2.0) probably corresponding to cysts or tissue necrosis, were visible in nine of the ten glioblastomas. The three meningiomas (Fig. 4) showed relatively high core MRGL between 21.7 and 40.1 μmol/100 g/min.

An improvement of the contrast of tumor MRGL between semibenign (grade II) and malignant (grade III and IV) gliomas was achieved by calculating ratios of tumor core through contralateral hemispheric MRGL (relative MRGL). This was due to a tendency towards lower MRGL values in contralateral brain tissue in patients with malignant gliomas; they were below the normal range (mean ± 2 s.d.) in three of ten patients with glioblastomas and one of four with grade III gliomas (Table 3). Grade III gliomas had a consistently higher relative MRGL than grade II gliomas, as illustrated in Figure 5. Relative MRGL in glioblastomas showed a broad overlap with grade II and III gliomas. Therefore, the overall correlation between tumor grade and relative tumor MRGL did not reach significance in this sample (Kendall's $\tau_B = 0.31$, $p = 0.08$).

Metabolism in gross regions, which also included the tumor borderzones and possibly parts of normal brain in some cases, were on average sligthly higher than core regions in grade II and III gliomas and meningiomas because of the high metabolism of gray matter structures in the tumor periphery. Only in glioblastomas, where extensive metabolic deactivation was found in adjacent structures (*23*) and necrotic tumor parts were frequently present, was gross tumor metabolism on average slightly lower than core MRGL.

Phosphorus-31 Spectra in Tumors

Usable ^{31}P spectra were recorded in all tumors and in homotopic contralateral tissue volumes. However, in four glioblastomas with large cystic compartments, the signal-to-noise ratio was low, impairing the evaluation of the relative height of individual peaks in comparison to the β-ATP used as the internal standard. This finding suggested decreased total amounts of energy-rich compounds in the tumor. For the various tumor groups, more or less typical spectra were found: P-31 spectra in astrocytomas grade II were usually not different from those in contralateral normal tissue (Fig. 1), only in one case was phosphocreatine slightly reduced, and in two instances PDEs were moderately diminished (Table 3). The pH in these tumors was in the normal range (7.01) and even slightly below the contralateral tissue. In all four grade III tumors, PCr and PDE were markedly reduced (Fig. 2) with increased and decreased phosphomonoester-peaks in one instance each (Table 3). Compared to normal control values and to the value measured contralaterally pH was shifted to the alkaline range (7.15). In the glioblastoma group, reduced PD peaks were the most frequent result (nine tumors) with split PD peaks in six instances (Fig. 3); reduced PCr occurred in five cases, whereas PM diminished in one and increased in two tumors (Table 3). In these tumors, pH was shifted to alkaline values (7.17), but pH in contralateral tissue (7.11) was also significantly different from control. All three meningiomas had decreased PDE peaks (Fig. 4); the most conspicuous finding in this group was a severe reduction of PCr to or below the level of ATP. Increased PME was found in one meningioma. Tumor pH was again in the alkaline range (7.16). There was no correlation between pH and MRGL in tumors (Fig. 6) and contralateral brain tissue.

DISCUSSION

Methodologic Aspects

While FDG-PET assesses the local turnover of glucose as the most important and nearly exclusive substrate of energy metabolism in the brain, ^{31}P-MRS estimates the tissue concentration of energy-rich phosphates as the endproduct of glycolysis and oxydation.

Additionally, MRS might indicate abnormal tissue metabolism leading to pH changes and might give some insight in pathologic alteration of membrane lipids as expressed in relative changes of the PMEs and PDEs. Based on this concept, the two methods would yield complementary information on different steps of the energy metabolism and could help to define the biologic activity of brain tumors.

The comparability of results obtained with the two methods, however, is still limited by their technical peculiarities, the most important being the different

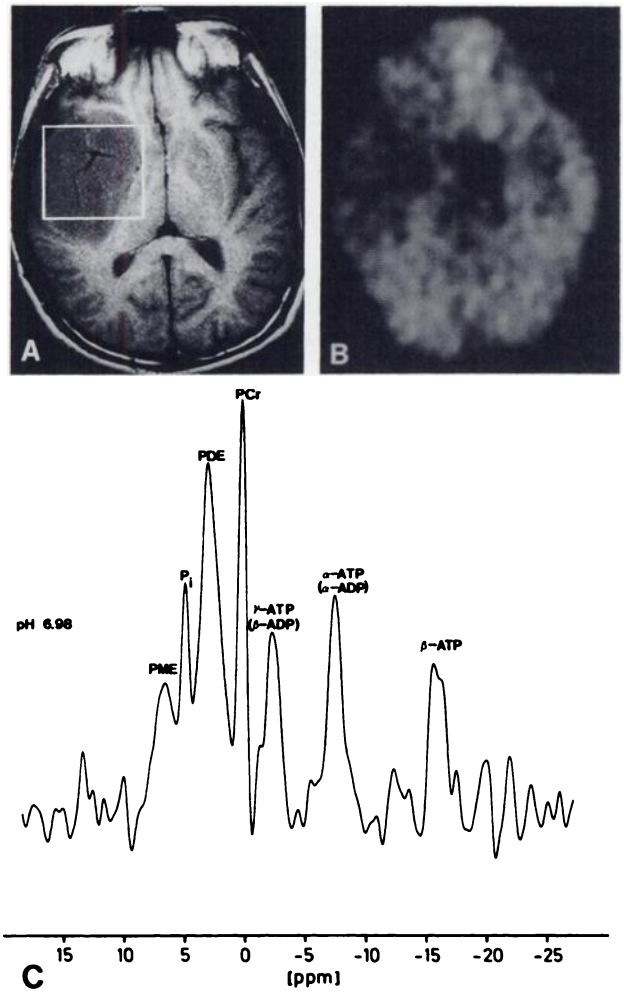

FIGURE 1
FDG-PET, MRI, and ^{31}P-MRS in a patient with a large right temporal astrocytoma II (all images are shown with patient's right side on viewer's left). (A) FDG-PET, ~ 27 mm above CML, showing low glucose metabolism (17 μmol/100 g/min) in tumor area (gray scale range, 5 to 55 μmol/100 g/min). (B) MRI (SE 250/30) for defining the volume of interest (50×50×50 mm) within the temporal space-occupying lesion. (C) Volume-selective ^{31}P-MRS within astrocytoma shows normal spectrum. The signals have been assigned to adenosine triphosphate (ATP), phosphocreatine (PCr), phosphodiesters (PDE), inorganic phosphate (Pi), and phosphomonoesters (PME). Intracellular pH calculated from the chemical shift of Pi versus PCr was 6.99.

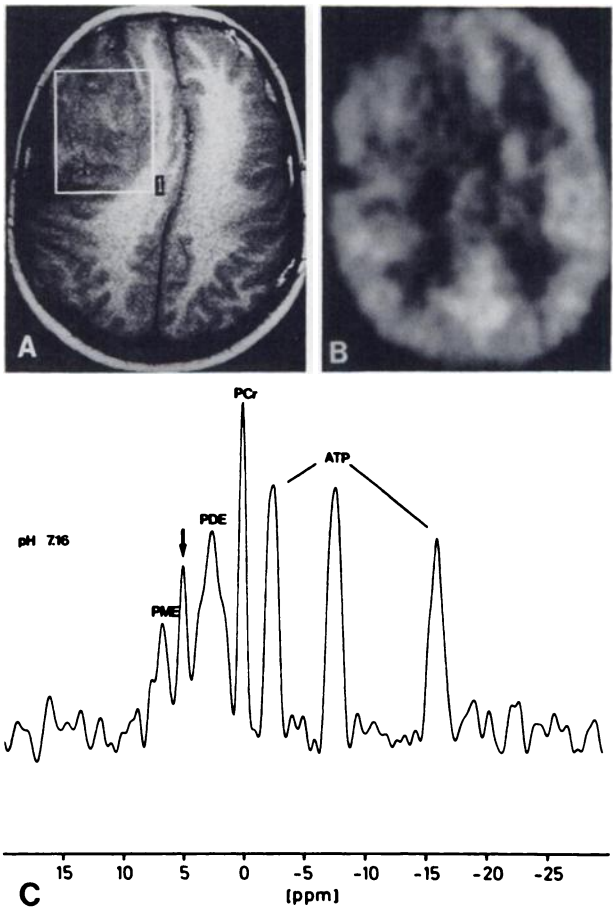

FIGURE 2
FDG-PET, MRI, and ^{31}P-MRS in a patient with right frontal astrocytoma grade III (A) FDG-PET, ~ 67 mm above CML, showing higher MRGl in the tumor core (mean 24 μmol/100 g/min) than in normal white matter, with a rim of low MRGl surrounding the tumor core (gray scale range, 5–60 μmol/100 g/min). (B) MRI demonstrates the mass effect of the large tumor. This study was used for defining the volume of interest (40×50×60 mm). (C) Compared to healthy tissue ^{31}P-MRS reveals reduced phosphodiesters and phosphocreatine. Determination of the pH value from the chemical shift of the Pi peak (arrow) indicates an alkaline environment in the tumor tissue.

spatial resolution. Due to the large amount of phosphorous (~ 30 cc) needed to obtain reliable ^{31}P signals in MRS, the various tissue compartments of brain tumors or pathologic changes below the selected excited volume cannot be resolved but are averaged. Consequently, typical changes in actively proliferating tissue may be hidden in the atypical spectra obtained from inactive, normal, or cystic compartments. Additionally, quantitation of tissue concentrations of various substrates is still impaired by inaccuracies in calibration and by the long time necessary for investigation (*9*, *24*). Therefore, usually only qualitative comparisons of the peak heights are used for clinical evaluations (*11*, *20*). The extended times for obtaining ^{1}H images to define normal and

pathologic morphology and for shimming the magnetic fields for volume selection for in vivo spectroscopy (*18*) hindered the recording of more than two spectra in one patient. However, this technical limitation will be solved in the near future (*25*, *26*).

On the other hand, FDG-PET has a better spatial resolution (7.8 mm FWHM with 11-mm slice thickness in the equipment used (*27*)) but still needs high resolution morphologic imaging (x-ray CT or ^{1}H-MRI) for definition of normal and pathologic tissue compartments. With this method, the various parts of heterogeneous tumors can be shown, and glucose uptake can be assessed in actively-proliferating tumor tissue and in necroses or cysts. With seven or fourteen contingent brain slices, the effect of a localized lesion on metabolism of the whole brain and in areas remote from the tumor can be quantified and functional depression, due probably more often to transneuronal interaction than

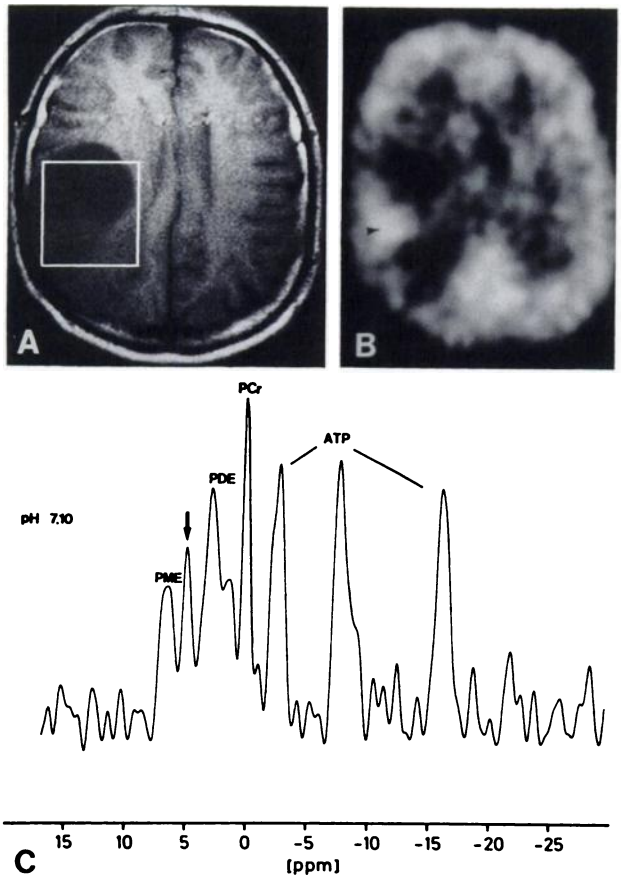

FIGURE 3
FDG-PET, MRI, and ^{31}P-MRS in a patient with right temporal glioblastoma (A) FDG-PET, ~ 54 mm above CML, showing an inhomogeneous tumor with high MRGL (peak value, 60 μmol/100 g/min) in tumor parts close to temporal convexity (arrowhead) and low MRGL (~ 5 μmol/100 g/min) in deeper tumor parts (gray scale range, 5–60 μmol/100 g/min). (B) Corresponding MRI with volume of interest. (C) Phosphorus-31 spectrum shows in particular reduction and possible splitting of PDEs, but also some decrease of the phosphocreatine signal. The tumor pH was 7.10.

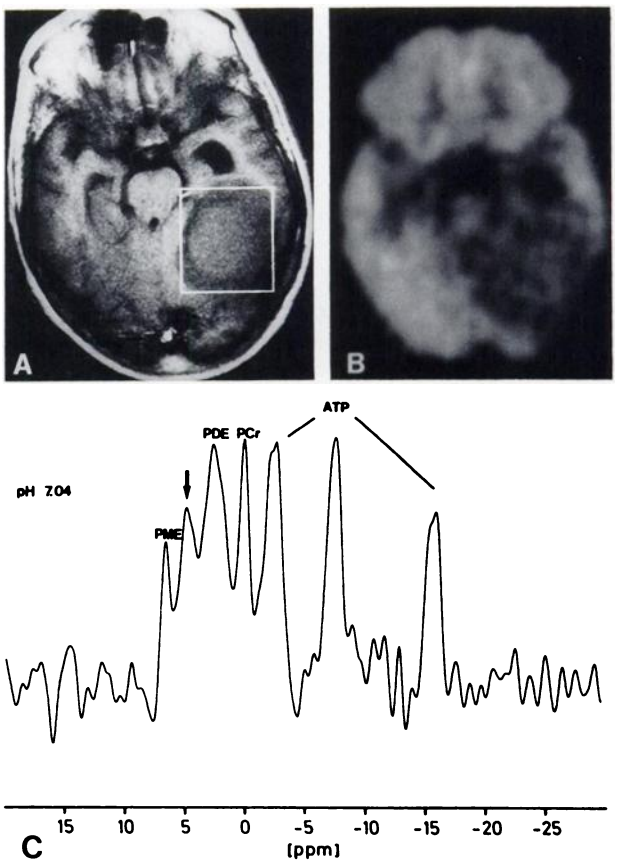

FIGURE 4
FDG-PET, MRI, and ^{31}P-MRS in a patient with meningioma at the left tentorium. (A) FDG-PET, ~ 27 mm above CML, showing intermediate (between normal gray and white matter) MRGL in tumor (tumor mean 22; gray scale range, 5 to 60 μmol/100 g/min). (B) MRI with volume of interest. (C) Phosphorus-31 spectrum of the tumor shows a drastic decrease of phosphocreatine to the level of adenosinetriphosphate and a reduction of phosphodiesters. In contrast to most examined meningiomas tumor pH is not shifted to the alkaline range.

to physical factors of the mass occupying lesion (*28*), can be demonstrated. As shown repeatedly in previous studies (*16*, *29*), the kinetic constants for the Sokoloff model vary in pathologic tissue and cause inaccuracies in the calculation of regional MRGL. Method insufficiencies can be overcome by kinetic determination of regional model constants and calculation of MRGL with these individually determined values. Such kinetic determinations of the MRGL using the method described by Herholz (*30*) were possible in 19 of the 24 patients in the present study. There was, however, no difference with respect to the metabolic classification of tumors and all other main findings of the study.

Another problem inherent in the determination of glucose metabolism with the FDG method is the possible difference of various hexoses with respect to transport and enzyme affinities in pathologic tissue. In order to correct for the differences between FDG and glucose, a standardized experimentally determined "lumped

TABLE 3
Frequency of Abnormal Findings

Histologic diagnosis	n	MRGL* increased	Necrosis in PET	pH†	Tumor PCR reduced	PME reduced	PME increased	PDE reduced	PDE split	Contralat. MRGL reduced	Brain pH†
Astrocytoma Grade II	6	1 (17%)	0	0	1 (17%)	0	0	2 (33%)	0	0	0 (of 5)
Glioma Grade III	4	3 (75%)	2 (50%)	3 (75%)	4 (100%)	1 (25%)	1 (25%)	4 (100%)	0	1 (25%)	0 (of 3)
Glioblastoma‡	10	1 (10%)	9 (90%)	7 (70%)	5 (50%)	1 (10%)	2 (20%)	9 (90%)	6 (60%)	3 (30%)	2 (of 8) (25%)
Meningioma	3	2 (67%)	0	2 (67%)	3 (100%)	0	1 (33%)	3 (100%)	0	0	1 (of 1)

* Above normal white matter MRGL (mean ± 2 s.d.).
† Exceeding normal hemispheric values (mean ± 2 s.d.).
‡ Poor signal-to-noise ratio in MR spectra of four cases.

constant" (*31*) is used for the calculation of MRGL. Dynamic PET studies of the distribution and accumulation of two different hexoses, FDG and ^{11}C-methylglucose (CMG) (*32*) have confirmed the preservation of the relation between active transport rate constants of CMG and FDG in pathologic tissue. However, different affinities of the tracers to hexokinase isoenzymes, as were shown for FDG and glucose in cultured tumor cells (*33*), cannot be ruled out completely, and, therefore, there remains a possible inaccuracy of the lumped constant as a source of incorrect MRGL values in tumorous tissue. In spite of these difficulties, an increase of hexokinase activity in relation to the degree of histologic differentiation of gliomas has been confirmed in in vitro studies by Timperley (*34*). The error introduced by mannose contamination of up to 50% in the FDG synthesis used (*14*) may result in an underestimation of absolute MRGL values by 8% (Wienhard K, Pawlik G, Nebeling B, unpublished data, 1990). However, the influence of such tracer impurities can be neglected when relative values are used.

Energy Metabolism of Tumors

In our small sample of mostly histologically verified brain tumors, a high variability of the absolute MRGL values was found in tumors precluding a clear relationship between MRGL and tumor grade. This result is similar to that of Tyler et al. (*6*), who also reported variable and often low MRGL in their small series of verified gliomas. A somewhat better differentiation between high-grade and low-grade gliomas was obtained by looking at the tumor core MRGL relative to contralateral MRGL, since malignant tumors tend to lower contralateral MRGL. Use of such relative metabolic values has been suggested by DiChiro (*1, 5*) on the basis of his experience in a much larger series of brain tumors.

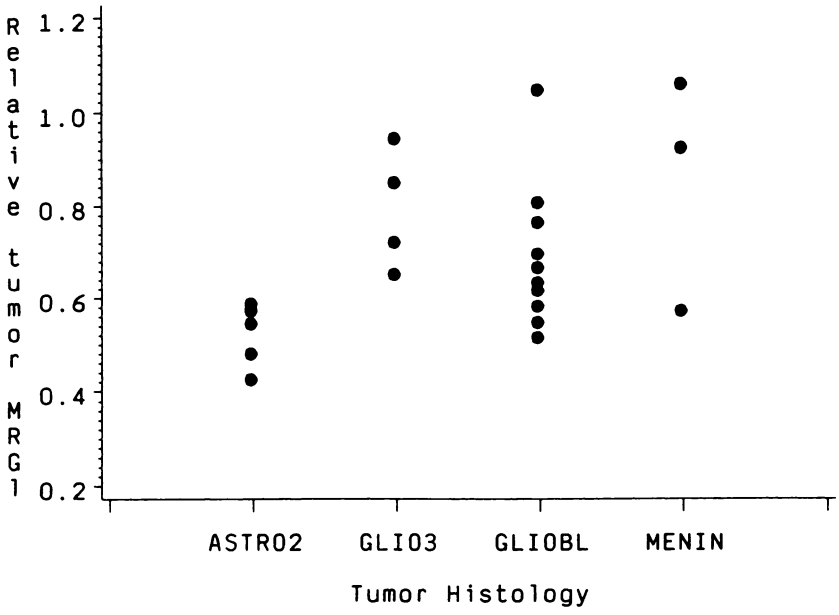

FIGURE 5
Plot of tumor core MRGL, relative to MRGL in the contralateral hemisphere, in the various histologic groups (ASTRO2 = astrocytomas grade II, GLIO3 = gliomas grade III, GLIOBL = glioblastomas, MENIN = Meningiomas). A broad overlap between histologic groups is demonstrated, with a tendency towards higher relative MRGL in high-grade gliomas in comparison with astrocytomas of grade II.

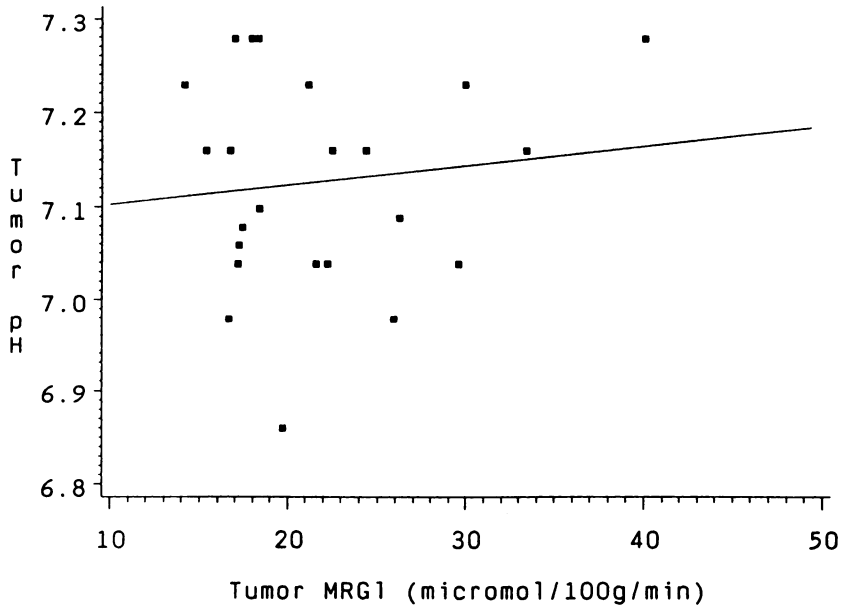

FIGURE 6
Scatter plot and linear regression line (ns) of tumor pH, measured with MRS, versus tumor core MRGL, measured with PET.

Yet, even the relative MRGL were often relatively low in glioblastomas (Fig. 5), limiting severely its usefulness as a single parameter for diagnostic purposes. This low metabolism is most likely due to regressive changes in glioblastomas, beginning at the microscopic level and expanding slowly to large necrotic and cystic parts, which can then be identified with PET as areas of very low metabolism. Correspondingly, marked inhomogeneity of MRGL within gliomas, i.e., very low values indicative of necrotic cysts and relatively high values suggesting actively proliferating tumor tissue, may also be taken as an indicator of malignancy.

Most astrocytomas of grade II showed no metabolic differences to normal brain tissue, i.e., mixed tissue in MRS and white matter in PET. This is consistent with their histologic composition of relatively normal astrocytes. The increase of glycolysis in grade III gliomas was obviously not accompanied by a higher accumulation of energy-rich phosphates; the PCr peak was rather reduced in comparison with normal brain. It may, therefore, be concluded that an increase of MRGL in malignant gliomas above normal white matter values is not sufficient to maintain homeostasis, but may rather correspond to severe derangement of energy metabolism. Thus, our findings do not support the suggestion of Warburg (*35*) that increased glycolysis to lactate may compensate for insufficient mitochondrial respiration in malignant tumors.

The MRGL values measured in the three meningiomas of this series are rather high in comparison to the values reported as characteristic for this tumor type (*1*, *36*). In some meningiomas, such high metabolic rates may indicate a tendency to malignant degeneration (*36*). While a high CMRGL also was observed in a meningo-sarcoma not included in this comparative study, the three meningiomas reported here had no histologic sign of malignancy, and the patients are in good condition without clinical or CT recurrencies since surgery.

pH in Tumors

It is a consistent finding in PET (*6*, *37–39*) and MRS studies (*11*, *20*) that tumor tissue is more alkaline than normal brain tissue. While there was no relationship of pH to metabolic rate of glucose in our cases—a tendency to higher pH with low metabolic rates was apparent in the study of Tyler et al. (*6*)—the various tumor groups showed different mean pH values with benign astrocytomas having a pH of normal brain tissue and high-grade gliomas and meningiomas being significantly alkaline (7.15–7.17). This yields another criterion for differential diagnosis of brain tumors. Surprisingly, in some glioblastomas the pH in the volume contralateral to the tumor also was significantly shifted to the alkaline range when compared to a normal control group (7.11 vs 7.01). Such an alkaline shift in contralateral nontumorous brain tissue could possibly be related to generalized edema with increased extracellular fluid volume.

Membrane Phosphates

The PMEs and PDEs contribute a large proportion of the ^{31}P signal in MRS. Phosphomonoesters, mostly phosphoethanolamine (*40*,*41*), and PDEs, mobile brain phospholipids like glycerol-phosphoryl-ethanol-amine and glycerol-phosphoryl-choline (*42*), are abundant in normal brain tissue and also in brain tumors. Therefore, their decrease in meningiomas might be expected. Since the cellular composition of benign astrocytomas is not grossly altered as compared to normal tissue, these constituents are at normal concentration or only slightly diminished in those tumors. In contrast, high-grade gliomas are characterized by heterogeneity of

tissue with necrotic and highly proliferating cellular compartments in close vicinity. Decreases of PDE and changes in their structure leading to splitting of PDE peaks could be caused by decomposition of membranous phospholipids in regions of tumor necrosis, but the changes in PDE and occasional increases of PME could also be due to induced biosynthesis of phospholipids in regions of rapid tumor growth. Although the underlying mechanisms remain unclear, the changes in PME and PDE peaks can contribute to the grading and differential diagnosis of brain tumors.

CONCLUSIONS

Our data indicate that measurement of the tumor MRGL alone does not permit differentiation between various types of brain tumors. The combination of MRGL measurement in tumor core relative to contralateral brain and visual evaluation of PET images with regard to presence of areas with extremely low metabolism leads to a better distinction between low-grade and high-grade gliomas. Differential diagnosis of brain tumors can be improved with additional ^{31}P-MRS, where low-grade gliomas usually show a normal spectrum, but high-grade gliomas are characterized by a variety of abnormalities such as reduced (and split) PDE, alkaline pH, and lowered PCr. Meningiomas as extraaxial lesions, are characterized above all by extremely low PCr, whereas their MRGL covers a wide range that prevents usage for diagnostic classification.

We found no direct relation between glycolysis and pH or the MRS findings. Since the two methods examine different aspects of abnormal tumor metabolism, both can contribute independently to the differential diagnosis of brain tumors and should be regarded as complementary tools for further elucidation of the complexities of tumor biology.

REFERENCES

1. DiChiro G. Positron emission tomography using (^{18}F)fluorodeoxyglucose in brain tumors. *Invest Radiol* 1987; 22:360–371.
2. Warburg O. *The metabolism of tumors.* New York: A. Constable; 1930.
3. Patronas NJ, DiChiro G, Kufta C, et al. Prediction of survival in glioma patients by means of positron emission tomography. *J Neurosurg* 1985; 62:816–822.
4. Alavi JB, Alavi A, Chawluk J, et al. Positron emission tomography in patients with glioma. *Cancer* 1988; 62:1074–1078.
5. DiChiro G, Brooks RA. PET-FDG of untreated and treated cerebral gliomas. *J Nucl Med* 1988; 29:421–422.
6. Tyler JL, Diksic M, Villemure JG, et al. Metabolic and hemodynamic evaluation of gliomas using positron emission tomography. *J Nucl Med* 1987; 28:1123–1133.
7. Herholz K, Ziffling P, Staffen W, et al. Uncoupling of hexose transport and phosphorylation in human gliomas demonstrated by PET. *Eur J Cancer Clin Oncol* 1988; 24:1139–1150.
8. Griffiths JR, Cady E, Edwards RHT, McCready VR, Wilkie DR, Wiltshaw E. ^{31}P-NMR studies of a human tumor in situ. *Lancet* 1983; I:1435–1436.
9. Oberhänsli RD, Bore PJ, Rampling RP, Hilton-Jones D, Hands LJ, Radda GK. Biochemical investigation of human tumors in vivo with phosphorus-31 magnetic resonance spectroscopy. *Lancet* 1986; II:8–11.
10. Segebarth CM, Balériaux DF, Arnold DL, Luyten PR, den Hollander JA. MR image-guided P-31 MR spectroscopy in the evaluation of brain tumor treatment. *Radiology* 1987; 165:215–219.
11. Heindel W, Bunke J, Glathe S, Steinbrich W, Mollevanger L. Combined ^{1}H-MR imaging and localized ^{31}P-spectroscopy of intracranial tumors in 43 patients. *J Comput Assist Tomogr* 1988; 12:907–916.
12. Heiss WD, Heindel W, Herholz K, Bunke J. Comparison of FDG-PET and image-guided P-31 MR-spectroscopy in brain tumors. *J Nucl Med* 1988; 29:785.
13. Ido T, Wan CN, Fowler JS. Fluorination with F_2: A convenient synthesis of 2-deoxy-2-fluoro-D-glucose. *J Org Chem* 1977; 42:2341–2342.
14. Ehrenkaufer RE, Potocki JE, Jewett DM. Simple synthesis of F-18-labeled-2-fluoro-2-deoxy-D-glucose: concise communication. *J Nucl Med* 1984; 25:333–337.
15. Heiss WD, Pawlik G, Herholz K, Wagner R, Göldner H, Wienhard K. Regional kinetic constants and CMRGlu in normal human volunteers determined by dynamic positron emission tomography of (^{18}F)-2-fluoro-2-deoxy-D-glucose. *J Cereb Blood Flow Metab* 1984; 4:212–223.
16. Wienhard K, Pawlik G, Herholz K, Wagner R, Heiss WD. Estimation of local cerebral utilization by positron emission tomography of (^{18}F)-2-fluoro-2-deoxy-D-glucose: a critical appraisal of optimization procedures. *J Cereb Blood Flow Metab* 1985; 5:115–125.
17. Herholz K, Pawlik G, Wienhard K, Heiss WD. Computer-assisted mapping in quantitative analysis of cerebral positron emission tomograms. *J Comput Assist Tomogr* 1985; 9:154–161.
18. Ordidge RJ, Connelly A, Lohman JAB. Image-selected in vivo spectroscopy (ISIS). A new technique for spatially selective NMR spectroscopy. *J Magn Reson* 1986; 66:283–294.
19. den Hollander JA, Luyten PR. Image-guided localized ^{1}H and ^{31}P-NMR spectroscopy of humans. *Ann NY Acad Sci* 1987; 508:386–398.
20. Arnold DL, Shoubridge EA, Feindel W, Villemure JG. Metabolic changes in cerebral gliomas within hours of treatment with intra-arterial BCNU demonstrated by phosphorus magnetic resonance spectroscopy. *Can J Neurol Sci* 1987; 14:570–575.
21. Moon RB, Richards JH. Determination of intracellular pH by ^{31}P magnetic resonance. *J Biol Chem* 1973; 248:7276–7278.
22. Petroff OAC, Prichard JW, Behar KL, Alger JR, den Hollander JA, Shulman RG. Cerebral intracellular pH by P-31 nuclear magnetic resonance spectroscopy. *Neurology* 1985; 35:781–788.
23. Alavi JB, Alavi A, Powe J, Hackney D, Reivich M. Metabolic and structural findings related to white matter disorders as shown by PET, MRI and CT. *J Nucl Med* 1986; 27:889–890.
24. Roth K, Hubesch B, Naruse S, et al. Quantitation of metabolites in human brain using volume-selected P-31 NMR. *J Magn Reson* 1987; 2:608.
25. Brown TR, Kincaid BM, Ugurbil K. NMR chemical shift imaging in three dimensions. *Proc Natl Acad Sci USA* 1982; 79:3523–3526.
26. Maudsley AA, Hilal SK, Perman WH, Simon HE. Spatially resolved high resolution spectroscopy by "four-dimensional"

NMR. *J Magn Reson* 1983; 51:147–152.
27. Eriksson L, Bohm C, Kesselberg M, et al. A four-ring camera system for emission tomography of the brain. *IEEE Trans Nucl Sci NS* 1982; 29:539–543.
28. DeLaPaz RL, Patronas NJ, Brooks RA, et al. A positron emission tomography (PET) study of suppression of glucose utilization in cerebral gray matter associated with brain tumor. *AJNR* 1983; 4:826–829.
29. Hawkins RA, Phelps ME, Huang SC. Effects of temporal sampling, glucose metabolic rates, and disruptions of the blood-brain barrier on the FDG model with and without a vascular compartment: studies in human brain tumors with PET. *J Cereb Blood Flow Metab* 1986; 6:170–183.
30. Herholz K. Non-stationary spatial filtering and accelerated curve fitting for parametric imaging with dynamic PET. *Eur J Nucl Med* 1988; 14:477–484.
31. Sokoloff L, Reivich M, Kennedy C, et al. The (^{14}C)deoxyglucose method for the measurement of local cerebral glucose utilization: theory, procedure, and normal values in the conscious and anesthetized albino rat. *J Neurochem* 1977; 28:897–916.
32. Herholz K, Wienhard K, Pietrzyk U, Pawlik G, Heiss WD. Measurement of blood-brain hexose transport with dynamic PET: comparison of (^{18}F)2-fluoro-2-deoxyglucose and (^{11}C)0-methylglucose. *J Cereb Blood Flow Metab* 1989; 9:104–110.
33. Dominguez JE, Graham JF, Cummins CJ, et al. Enzymes of glucose metabolism in cultured human gliomas: neoplasia is accompanied by altered hexokinase, phosphofructokinase, and glucose-6-phosphate dehydrogenase levels. *Metab Brain Dis* 1987; 2:17–30.
34. Timperley WR. Glycolysis in neuroectodermal tumours. In: Thomas GDT, Graham DI, eds. *Brain tumours.* London: Butterworths; 1980:145–167.
35. Warburg O. On the origin of cancer cells. *Science* 1956; 123:309–314.
36. DiChiro G, Hatazawa J, Katz DA, et al. Glucose utilization by intracranial meningiomas as an index of tumor aggressivity and probability of recurrence: a PET study. *Radiology* 1987; 164:521–526.
37. Rottenberg DA, Ginos JZ, Kearfott KJ, Junck L, Dhawan V, Jarden JO. In vivo measurement of brain tumor pH using (^{11}C)DMO and positron emission tomography. *Ann Neurol* 1985; 17:70–79.
38. Arnold JB, Junck L, Rottenberg DA. In vivo measurement of regional brain and tumor pH using (^{14}C)dimethyloxazolidinedione and quantitative autoradiography. *J Cereb Blood Flow Metab* 1985; 5:369–375.
39. Brooks DJ, Beaney RP, Thomas DGT, Marshall J, Jones T. Studies on regional cerebral pH in patients with cerebral tumours using continuous inhalation of $^{11}CO_2$ and positron emission tomography. *J Cereb Blood Flow Metab* 1986; 6:529–535.
40. Prichard JW, Alger JR, Behar KL, Petroff OAC, Shulman RG. Cerebral metabolic studies in vivo by ^{31}P NMR. *Proc Natl Acad Sci USA* 1983; 80:2748–2751.
41. Brenton DP, Garrod PJ, Krywawych S, et al. Phosphoethanolamine is major constituent of phosphomonoester peak detected by ^{31}P NMR in newborn brain. *Lancet* 1985; I:115.
42. Cerdan S, Subramanian HV, Hilberman M, et al. P-31 NMR detection of mobile dog brain phospholipids. *Magn Reson Med* 1986; 3:432–439.